23rd ABCM International Congress of Mechanical Engineering
December 6-11, 2015, Rio de Janeiro, RJ, Brazil

# NUMERICAL SOLUTION OF THE GIESEKUS MODEL FOR TWO-DIMENSIONAL FLOWS

**Matheus T. Araujo**
**Murilo F. Tomé**
Institute of Mathematics and Computer Science - University of São Paulo, São Carlos, São Paulo, Brazil
mtaraujo@icmc.usp.br, murilo@icmc.usp.br

***Abstract.*** *This work presents a numerical method to simulate two-dimensional viscoelastic flows governed by the Giesekus constitutive equation. The governing equations are solved by the finite difference method on a staggered grid. The calculation of velocity and pressure is performed by an implicit method of second order in space and first order in time, while the Giesekus constitutive equation is solved by a second-order Runge-Kutta method. To verify the proposed numerical method, the authors develop an analytic solution for the steady flow of a Giesekus fluid between two parallel plates. Convergence results are provided by the use of mesh refinement.*

***Keywords:*** *Viscoelastic flows, Giesekus model, Finite difference, Analytic solution*

## 1. INTRODUCTION

The numerical simulation of flows of viscous fluids has been the subject of constant research in many international centres in the world. The research has been focused on the computational rheology area and numerical methods to simulate flows of Oldroyd-B, PTT, Giesekus, Upper-Convected Maxwell (UCM) fluids, among others, have been developed (McKee *et al.*, 2008; Alves *et al.*, 2001). The interest in the Giesekus model lies in the fact that this equation can predict first and second normal stress differences in important industrial flows. The numerical methods for simulating flows governed by this equation have employed the finite element method (Delvaux and Crochet, 1990; Oztekin *et al.*, 1994; Joie and Graebling, 2013; Mu *et al.*, 2013) and the application of this model to free surface flows has received little attention from the CFD comunity (e.g. Delvaux and Crochet (1990); Mu *et al.* (2013)). However, it is known that the existing methods for solving viscoelastic flows possess instabilities or even fail to predict flows of high elastic fluids. Notwithstanding, several investigators have studied this model and found analytic solutions for steady flows. For instance, Raisi *et al.* (2008), considered the developed flow of a Giesekus fluid between two parallel plates where the top plate is moving. These authors presented approximate solutions of the equations for $0 < \alpha < 1$ for a given value of the pressure gradient $dp/dx$. Steady Poiseuille flow was considered in the work of Schleiniger and Weinacht (1991) in which the authors solved the equations from the flow of a Giesekus fluid with a solvent viscosity and the solutions are obtained by solving a boundary value problem. There are other works that deal with analytic solution of the Giesekus model in which the solutions are restricted to specific values of the parameter $\alpha$ or consider a channel with a moving wall.

In this paper, we present a numerical methodology for solving the governing equations for two-dimensional flows governed by the constitutive equation Giesekus (Rajagopalan *et al.*, 1990). We propose to solve this equation using finite differences employing the modified Euler method. To verify the proposed numerical method, the authors develop an analytic solution for fully developed flows of a Giesekus fluid in a channel. This analytic solution is devised in a manner that the numerical solutions obtained are easily comparable with the corresponding analytic values. Convergence of the results is made by the use of mesh refinement.

## 2. BASIC EQUATIONS

The governing equations that describe isothermic incompressible flows can be described by the continuity and momentum equations which, in dimensionless form, can be written as:

$$\nabla \cdot \mathbf{u} = 0, \tag{1}$$

$$\frac{\partial \mathbf{u}}{\partial t} = -\nabla p + \nabla \cdot \boldsymbol{\tau} + \frac{1}{Fr^2}\mathbf{g}, \tag{2}$$

where $\mathbf{u} = (u, v)$ is the velocity vector, $p$ is the pressure, $\mathbf{g}$ is the gravitational field and $\boldsymbol{\tau}$ is the extra-stress tensor that obeys the Giesekus constitutive model and can be written as

$$\frac{\partial \boldsymbol{\tau}}{\partial t} = -\nabla \cdot (\mathbf{u}\boldsymbol{\tau}) + (\nabla \mathbf{u})\boldsymbol{\tau} + \boldsymbol{\tau}(\nabla \mathbf{u})^T + \frac{1}{Wi}\Big[-\boldsymbol{\tau} - \frac{\alpha Re Wi}{1-\beta}(\boldsymbol{\tau}\cdot\boldsymbol{\tau}) + \frac{2(1-\beta)}{Re}\mathbf{D}\Big], \quad \mathbf{D} = \frac{1}{2}[(\nabla \mathbf{u}) + (\nabla \mathbf{u})^T], \tag{3}$$

where $\alpha$ represents the mobility parameter that regulates de shear shinning fluid behavior ($0 \leq \alpha \leq 1$) and the parameter $\beta$ is the ratio of the viscosity of the solvent to the total viscosity of the fluid.

In equations Eq. (2)-Eq. (3), $Re = \dfrac{UL}{\nu}$, $Wi = \dfrac{\lambda U}{L}$ and $Fr = \dfrac{U}{\sqrt{gL}}$ denote, respectively, the Reynolds, the Weissenberg and the Froude numbers. $\nu = \eta/\rho$ represents the kinematic viscosity and $\lambda$ is the relaxation time of the fluid. $U$ and $L$ are velocity and length scales, respectively. Details of the nondimensionalisation of the equations are given in Araujo (2015).

### 2.1 Boundary conditions

To solve equations Eq. (1) and Eq. (2), it is necessary to impose some conditions for the velocity vector $\mathbf{u}$. For fluid entrances (inflows) the normal velocity is specified by $U = U_{inf}$ while at fluid exits (outflows) the Neumann condition $\dfrac{\partial \mathbf{u}}{\partial n} = \mathbf{0}$ is adopted, where $n$ represents the normal direction to the contour. At rigid boundaries the no-slip condition $\mathbf{u} = \mathbf{0}$ is imposed.

## 3. ANALYTIC SOLUTION

We consider a 2D-channel having unity width and fully developed flows, where $\mathbf{u} = (u(y), 0)$, $\dfrac{\partial p}{\partial x} = p_x = \text{constant}$, $\tau^{xy}(y), \tau^{yy}(y), \tau^{xx}(y),\ y\ \in\ [0,\ 1]$. In this case, the momentum equations Eq. (2) reduce to

$$\tau^{xy}_y = p_x, \tag{4}$$
$$\tau^{yy}_y = p_y, \tag{5}$$

and the Giesekus equation can be written as

$$\tau^{yy} + \alpha\mathbf{K}[(\tau^{yy})^2 + (\tau^{xy})^2] \quad = \quad 0, \tag{6}$$
$$u_y\tau^{yy} - \frac{1}{Wi}\Big\{\tau^{xy} + \alpha\mathbf{K}[\tau^{xy}(\tau^{xx} + \tau^{yy})]\Big\} + \frac{1}{\mathbf{K}}u_y \quad = \quad 0, \tag{7}$$
$$2u_y\tau^{xy} - \frac{1}{Wi}\Big\{\tau^{xx} + \alpha\mathbf{K}[(\tau^{xy})^2 + (\tau^{xx})^2]\Big\} \quad = \quad 0. \tag{8}$$

where $u_y(y) = \dfrac{\partial u}{\partial y}$ and $\mathbf{K} = \dfrac{ReWi}{1-\beta}$. Equations (4) - (8) must be solved for the unknowns $u_y, p_x, \tau^{xy}, \tau^{yy}$ and $\tau^{xx}$. These solutions are found as follows.

By integrating Eq. (4) over the interval $[0,\ y]$, the shear stress $\tau^{xy}$ is given by

$$\tau^{xy} = \int_0^y p_x ds = p_x y - \frac{1}{2}p_x, \quad y\ \in [0,\ 1]\ \text{ (the condition } \tau^{xy} = 0 \text{ when } y = 1/2 \text{ was employed) .} \tag{9}$$

Now, using Eq. (6), which is a second order algebraic equation in $\tau^{yy}$, we can evaluate $\tau^{yy}$ from

$$\tau^{yy} = \frac{-1 + \sqrt{1 - 4\alpha^2\mathbf{K}^2(\tau^{xy})^2}}{2\alpha\mathbf{K}}, \quad \text{where we must have} \quad 1 - 4\alpha^2\mathbf{K}^2(\tau^{xy})^2 \geq 0, \quad \text{for real solutions.} \tag{10}$$

In this equation, the positive sign of the root was chosen so $\tau^{yy} = 0$ in the middle of channel and it must also give $\tau^{yy} = 0$ if $\alpha = 0$ in Eq. (6), corresponding to the UCM model. More about the choice of this solution can be seen in Schleiniger and Weinacht (1991).

The solution given by Eq. (10) permits us to evaluate $\dfrac{\partial u}{\partial y} = u_y$ from Eq. (7) as

$$u_y = \frac{1}{Wi}\Big(\frac{\tau^{xy}}{\tau^{yy} + \frac{1}{\mathbf{K}}}\Big)\Big[1 + \alpha\mathbf{K}(\tau^{xx} + \tau^{yy})\Big] \tag{11}$$

which introduced into Eq. (8), produces

$$\Big\{2\Big(\frac{(\tau^{xy})^2}{\tau^{yy} + \frac{1}{\mathbf{K}}}\Big)\Big[1 + \alpha\mathbf{K}(\tau^{xx} + \tau^{yy})\Big]\Big\} - \Big\{\tau^{xx} + \alpha\mathbf{K}\big[(\tau^{xy})^2 + (\tau^{xx})^2\big]\Big\} = 0. \tag{12}$$

This is a second order algebraic equation in $\tau^{xx}$ which has 2 solutions. The solution chosen for $\tau^{xx}$ is one that gives a positive first normal stress difference ($N_1 = \tau^{xx} - \tau^{yy} > 0$), in the middle of the channel and is given by

$$\tau^{xx} = \frac{-B - \sqrt{B^2 - 4AC}}{2A} \tag{13}$$

where

$$A = -\alpha\, K, \quad B = 2\big(\tau^{xy}\big)^2\left[\frac{\alpha K}{\tau^{yy} + \frac{1}{K}}\right] - 1, \quad C = (\tau^{xy})^2\left[\frac{2}{\tau^{yy} + \frac{1}{K}}\big(1 + \alpha K \tau^{yy}\big) - \alpha K\right]$$

Therefore, $\tau^{xy}$ and $\tau^{yy}$ are computed from Eq. (9) and Eq. (10) while $\tau^{xx}$ is obtained from Eq. (13) and finally, $u_y$ is evaluated using Eq. (11). However, these solutions depend on the value of $p_x$ which is calculated in the next section.

### 3.1 Calculation of $p_x$

To evaluate equations Eq. (9)-Eq. (13), the value of $p_x$ is required. It is obtained as follows: at the channel entrance, a Newtonian parabolic profile $u_{inf}(y)$ is imposed which gives $\int_0^1 u_{inf}(y)dy = 2/3$ so the Giesekus solution $u(y)$ must also provide $\int_0^1 u(y)dy = 2/3$ and integration by parts and the no-slip condition for $u(y)$, yields the following equation

$$\int_0^1 y\, u_y dy + 2/3 = 0, \quad \text{where } u_y \text{ is given by Eq. (11)}\,. \tag{14}$$

Equation (14) is a nonlinear equation for the unknown $p_x$ and can be solved by many iterative methods for solving roots of nonlinear equations. In this work we chose to calculate $p_x$ by the bissection method. Having calculated $p_x$, the velocity $u(y)$ is obtained by integrating $u_y(y)$ over the interval $[0,\ 1]$. For details see Araujo (2015).

## 4. NUMERICAL METHOD

To solve equations Eq. (1) and Eq. (2), we first employ the EVSS (Elastic Viscous Stress Splitting) (Rajagopalan *et al.*, 1990) given by

$$\boldsymbol{\tau} = \frac{2}{Re}\boldsymbol{D} + \boldsymbol{T}, \tag{15}$$

where $\mathbf{T}$ is a non-Newtonian tensor that is reponsible for the elastic effects on the flow. With this transformation, the momentum equation Eq. (2) is transformed into equation

$$\frac{\partial \mathbf{u}}{\partial t} = -\nabla\cdot(\mathbf{u}\mathbf{u}) - \nabla p + \frac{1}{Re}\nabla^2\mathbf{u} + \nabla\cdot\mathbf{T} + \frac{1}{Fr^2}\mathbf{g}. \tag{16}$$

Equations Eq. (16) and Eq. (1) are solved by the finite difference method on a staggered grid using the implicit Euler technique presented in Oishi *et al.* (2011). Once the velocity and pressure are calculated, the extra-stress tensor is obtained by solving the Giesekus equation as follows.

The solutions $\mathbf{u}(\mathbf{x}, t_{n+1})$, $p(\mathbf{x}, t_{n+1})$ and $\boldsymbol{\tau}(\mathbf{x}, t_{n+1})$ at time $t_{n+1} = t_n + \delta t$ are obtained in two parts. First, using $\tau(\mathbf{x}, t_n)$, the velocity and the pressure are calculated at time $t_{n+1}$. Then, $\mathbf{u}(\mathbf{x}, t_{n+1})$ is employed to compute $\boldsymbol{\tau}(\mathbf{x}, t_{n+1})$ by the finite difference method using the modified Euler method. The details of the calculation of $\mathbf{u}(\mathbf{x}, t_{n+1})$, $p(\mathbf{x}, t_{n+1})$ can be found in Oishi *et al.* (2011) and is not given here. Next we describe the technique employed to calculate $\boldsymbol{\tau}(\mathbf{x}, t_{n+1})$.

### 4.1 Calculation of $\boldsymbol{\tau}(\mathbf{x}, t_{n+1})$

To calculate $\boldsymbol{\tau}(\mathbf{x}, t_{n+1})$ we write Eq. (3) for two-dimensional Cartesian flows in the form

$$\left\{\begin{aligned} &\frac{\partial \tau^{xx}}{\partial t} = \mathcal{G}^{xx}(\mathbf{u}, \boldsymbol{\tau}),\\ &\mathcal{G}^{xx}(\mathbf{u}, \boldsymbol{\tau}) = 2\Big(\frac{\partial u}{\partial x}\tau^{xx} + \frac{\partial u}{\partial y}\tau^{xy}\Big) - \Big(\frac{\partial(u\tau^{xx})}{\partial x} + \frac{\partial(v\tau^{xx})}{\partial y}\Big)\\ &\qquad -\frac{1}{Wi}\Big\{\tau^{xx} + \frac{\alpha ReWi}{1-\beta}[(\tau^{xx})^2 + (\tau^{xy})^2]\Big\} + \frac{2(1-\beta)}{ReWi}\frac{\partial u}{\partial x}, \end{aligned}\right. \tag{17}$$

$$\begin{cases} \dfrac{\partial \tau^{xy}}{\partial t} = \mathcal{G}^{xy}(\mathbf{u},\boldsymbol{\tau}), \\ \mathcal{G}^{xy}(\mathbf{u},\boldsymbol{\tau}) = \dfrac{\partial u}{\partial x}\tau^{xy} + \dfrac{\partial u}{\partial y}\tau^{yy} + \dfrac{\partial v}{\partial x}\tau^{xx} + \dfrac{\partial v}{\partial y}\tau^{xy} - \Big(\dfrac{\partial (u\tau^{xy})}{\partial x} + \dfrac{\partial (v\tau^{xy})}{\partial y}\Big) \\ \qquad -\dfrac{1}{Wi}\Big\{\tau^{xy} + \dfrac{\alpha ReWi}{1-\beta}[\tau^{xx}\tau^{xy} + \tau^{xy}\tau^{yy}]\Big\} + \dfrac{(1-\beta)}{ReWi}\Big(\dfrac{\partial u}{\partial y} + \dfrac{\partial v}{\partial x}\Big), \end{cases} \tag{18}$$

$$\begin{cases} \dfrac{\partial \tau^{yy}}{\partial t} = \mathcal{G}^{yy}(\mathbf{u},\boldsymbol{\tau}), \\ \mathcal{G}^{yy}(\mathbf{u},\boldsymbol{\tau}) = 2\Big(\dfrac{\partial v}{\partial x}\tau^{xy} + \dfrac{\partial v}{\partial y}\tau^{yy}\Big) - \Big(\dfrac{\partial (u\tau^{yy})}{\partial x} + \dfrac{\partial (v\tau^{yy})}{\partial y}\Big) \\ \qquad -\dfrac{1}{Wi}\Big\{\tau^{yy} + \dfrac{\alpha ReWi}{1-\beta}[(\tau^{xy})^2 + (\tau^{yy})^2]\Big\} + \dfrac{2(1-\beta)}{ReWi}\dfrac{\partial v}{\partial y}, \end{cases} . \tag{19}$$

The solution $\boldsymbol{\tau}(\mathbf{x}, t_{n+1})$ is obtained in two steps, as follows.

- Compute $\overline{\tau^{xx}}(\mathbf{x}, t_{n+1}), \overline{\tau^{yy}}(\mathbf{x}, t_{n+1}), \overline{\tau^{xy}}(\mathbf{x}, t_{n+1})$ by using equations

$$\overline{\tau^{xx}}(\mathbf{x}, t_{n+1}) = \tau^{xx}(\mathbf{x}, t_n) + \delta t \mathcal{G}^{xx}(\mathbf{u}^{(n+1)}, \boldsymbol{\tau}(\mathbf{x}, t_n)) \tag{20}$$
$$\overline{\tau^{yy}}(\mathbf{x}, t_{n+1}) = \tau^{yy}(\mathbf{x}, t_n) + \delta t \mathcal{G}^{yy}(\mathbf{u}^{(n+1)}, \boldsymbol{\tau}(\mathbf{x}, t_n)) \tag{21}$$
$$\overline{\tau^{xy}}(\mathbf{x}, t_{n+1}) = \tau^{xy}(\mathbf{x}, t_n) + \delta t \mathcal{G}^{xy}(\mathbf{u}^{(n+1)}, \boldsymbol{\tau}(\mathbf{x}, t_n)) \tag{22}$$

- Calculate $\tau^{xx}(\mathbf{x}, t_{n+1}), \tau^{yy}(\mathbf{x}, t_{n+1}), \tau^{xy}(\mathbf{x}, t_{n+1})$ by equations

$$\tau^{xx}(\mathbf{x}, t_{n+1}) = \tau^{xx}(\mathbf{x}, t_n) + \frac{\delta t}{2}\Big[\mathcal{G}^{xx}(\mathbf{u}^{(n+1)}, \boldsymbol{\tau}(\mathbf{x}, t_n)) + \mathcal{G}^{xx}(\mathbf{u}^{(n+1)}, \overline{\boldsymbol{\tau}}(\mathbf{x}, t_{n+1}))\Big] \tag{23}$$

$$\tau^{yy}(\mathbf{x}, t_{n+1}) = \tau^{yy}(\mathbf{x}, t_n) + \frac{\delta t}{2}\Big[\mathcal{G}^{yy}(\mathbf{u}^{(n+1)}, \boldsymbol{\tau}(\mathbf{x}, t_n)) + \mathcal{G}^{yy}(\mathbf{u}^{(n+1)}, \overline{\boldsymbol{\tau}}(\mathbf{x}, t_{n+1}))\Big] \tag{24}$$

$$\tau^{xy}(\mathbf{x}, t_{n+1}) = \tau^{xy}(\mathbf{x}, t_n) + \frac{\delta t}{2}\Big[\mathcal{G}^{xy}(\mathbf{u}^{(n+1)}, \boldsymbol{\tau}(\mathbf{x}, t_n)) + \mathcal{G}^{xy}(\mathbf{u}^{(n+1)}, \overline{\boldsymbol{\tau}}(\mathbf{x}, t_{n+1}))\Big] \tag{25}$$

As funções $\mathcal{G}^{xx}(\mathbf{u},\boldsymbol{\tau}), \mathcal{G}^{yy}(\mathbf{u},\boldsymbol{\tau}), \mathcal{G}^{xy}(\mathbf{u},\boldsymbol{\tau})$ são obtidas por meio das equações Eq. (17)-Eq. (19).

## 5. Verification of the methodology

To verify the implementation of the numerical method presented in this work, we simulated the flow in a two-dimensional channel of width $L$ and length $10L$ as illustrated in Fig. 1(a). The following data were employed:

- Inflow velocity: $U = 0.1ms^{-1}$, Lenght scale: $L = 0.01m$, Gravitational acceleration: $g = 0$
- Fluid definition: $\eta = 1$Pa.s, $\rho = 1000$kgm$^{-3}$, Giesekus parameters: $\alpha = 0.1$, $\beta = 0$, $\lambda = 0.04s$

With these data, we have $Re = UL/\nu = 1.0$ and $Wi = \lambda U/L = 0.4$.

With the objective to analyze the convergence of the numerical method, this problem was simulated in five different meshes: Mesh **M1** with $(10 \times 100)$ cells ($\delta_x = \delta_y = 0.001$), Mesh **M2** with $(20 \times 200)$ cells ($\delta_x = \delta_y = 0.0005$), Mesh **M3** with $(30\times 300)$ cells ($\delta_x = \delta_y = 0.00033$), Mesh **M4** with $(40\times 400)$ cells ($\delta_x = \delta_y = 0.00025$) and Mesh **M5** with $(50 \times 500)$ cells ($\delta_x = \delta_y = 0.0002$), until time $t = 100s$, where it is expected that steady state has been reached. The numerical values were computed at cell centres $(i_{out}, j)$, where $i_{out}$ denotes the index of a cell preceding the channel exit (outflow boundary).

Figure 1(b) displays the convergence of the pressure gradient values $p_x$ calculated on meshes **M1**, **M2**, **M3**, **M4** and **M5** which are compared to the value obtained using the Bissection method which is the analytic value obtained from Eq. (14). The numerical values were calculated by the second order formula $\dfrac{\partial p}{\partial x}\Big|_{i_{out}+\frac{1}{2}} = \dfrac{p_{i_{out},j} - p_{i_{out}-1,j}}{\delta x}$. It can be seen that as the mesh is refined the approximate values converge to the analytic value of $p_x$.

Figure 2 and Fig. 3 show the comparison between the numerical and the analytic solutions of $u(y)$, $\tau^{xx}(y)$, $\tau^{xy}(y)$, $\tau^{yy}(y)$ and $\dfrac{\partial u}{\partial y}(y)$, plotted on a cross section before the channel exit (see $i_{out}$ in Fig. 1(a)). We can observe that the agreement between the two solutions is excelent which verifies the numerical method for solving the Giesekus model.

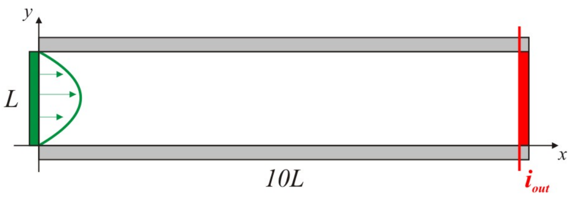


(a)

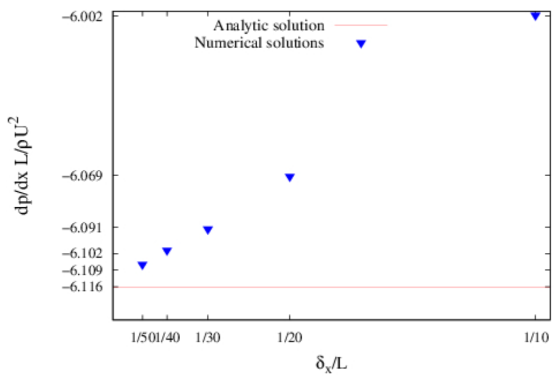


(b)

Figure 1. Convergence of the numerical values of the $dp/dx$ to the analytic value. (a) Description of the channel employed: channel entrance (green color), channel exit (red color); (b) Numerical values of $dp/dx$ obtained on various meshes.

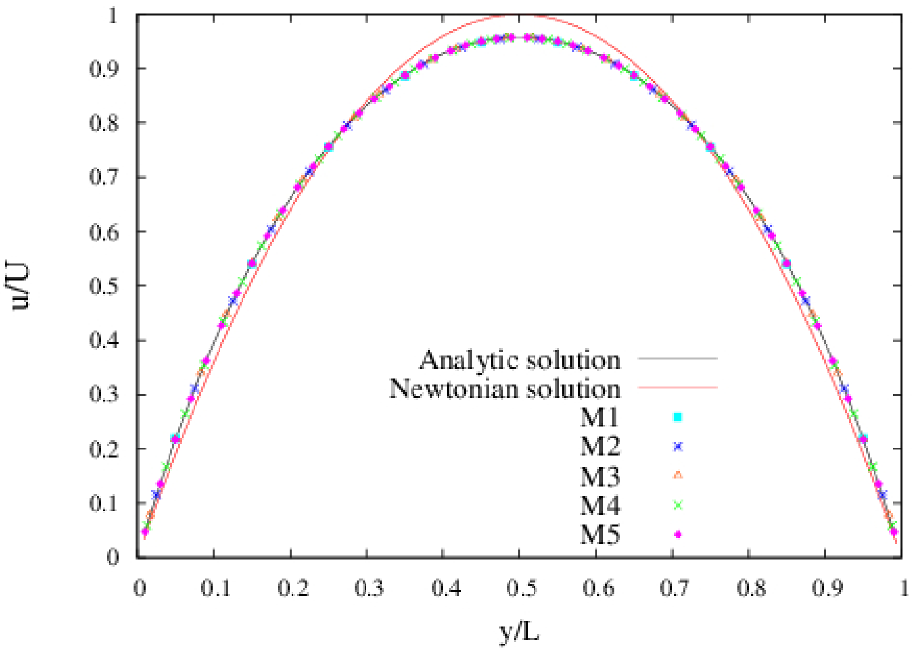


Figure 2. Comparison of analytic velocity and the numerical velocities obtained in meshes **M1**, **M2**, **M3**, **M4** and **M5**. For reference, the Newtonian velocity profile is also shown.

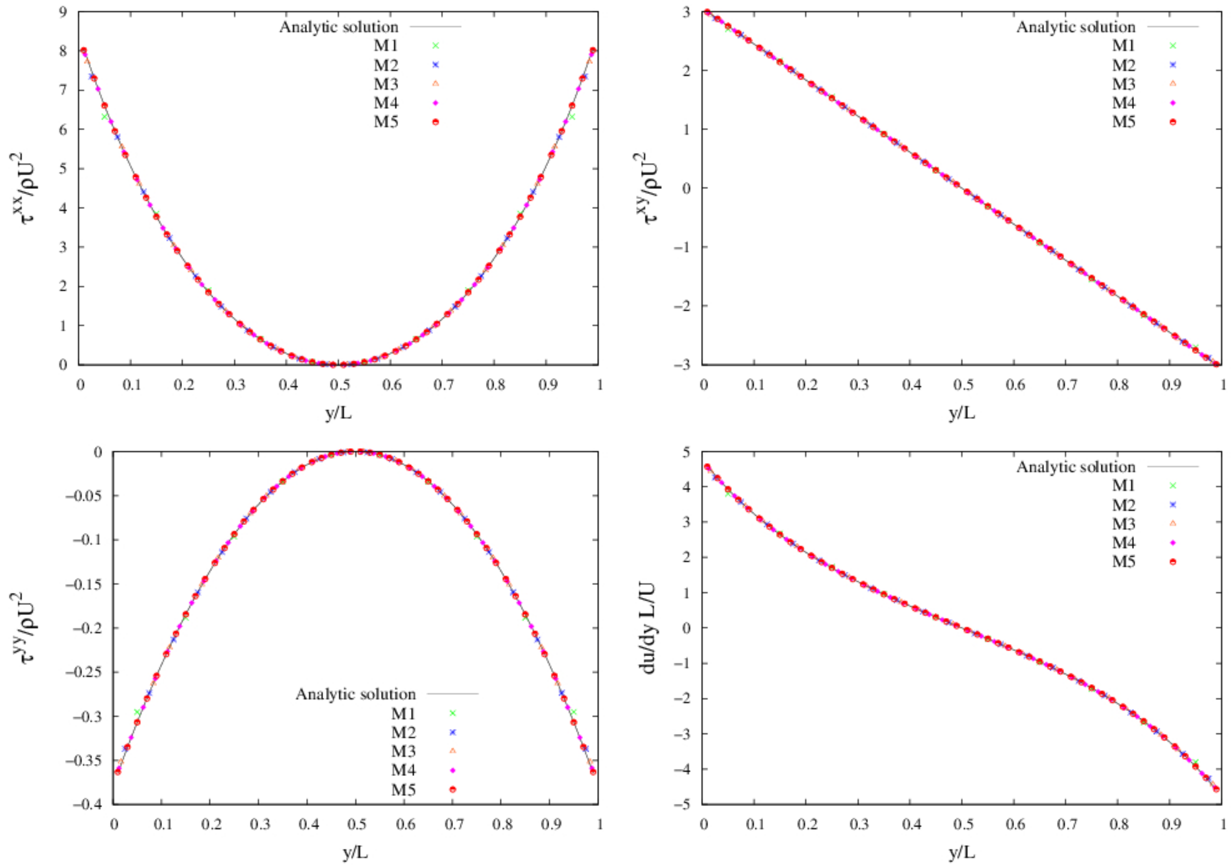


Figure 3. Comparison of the analytic and the numerical solutions obtained in meshes **M1**, **M2**, **M3**, **M4** and **M5**. a) $\tau_{xx}$ tensor, b) $\tau_{xy}$ tensor, c) $\tau_{yy}$ tensor and d) velocity variation $du/dy$.

To demonstrate the convergence of the numerical method, the relative errors obtained on the five meshes were computed by the formula

$$E = \sqrt{\frac{\sum_{ij}\left(ExSol - NumSol\right)^2}{\sum_{ij}\left(ExSol\right)^2}} \quad \text{where } ExSol \text{ represents the exact solution.} \tag{26}$$

Table 1 displays the errors obtained on the five meshes while Fig. 4 shows the decrease of the errors with mesh spacing $h$. We can see in Tab. 1 that the errors decrease with mesh refinement, becoming very small of order 1%. These results confirm that the numerical method developed in this work is convergent.

Table 1. Relative errors obtained on meshes **M1**, **M2**, **M3**, **M4** and **M5**.

| *Relative error* | *Meshes* | | | | |
|---|---|---|---|---|---|
| | **M1** | **M2** | **M3** | **M4** | **M5** |
| $E(\tau_{xx})$ | 3.690x10$^{-2}$ | 1.188x10$^{-2}$ | 5.408x10$^{-3}$ | 2.982x10$^{-3}$ | 1.850x10$^{-3}$ |
| $E(\tau_{xy})$ | 1.516x10$^{-2}$ | 4.131x10$^{-3}$ | 1.825x10$^{-3}$ | 1.012x10$^{-3}$ | 6.400x10$^{-4}$ |
| $E(\tau_{yy})$ | 3.265x10$^{-1}$ | 1.009x10$^{-2}$ | 4.533x10$^{-3}$ | 2.488x10$^{-3}$ | 1.543x10$^{-3}$ |
| $E(du/dy)$ | 2.585x10$^{-2}$ | 8.354x10$^{-3}$ | 3.827x10$^{-3}$ | 2.120x10$^{-3}$ | 1.320x10$^{-3}$ |

## 6. CONCLUSIONS

This work presented a numerical technique to simulate viscoelastic fluid flows governed by the constitutive equation Giesekus. The developed numerical method employs the finite difference method on a staggered grid. The momentum equations are solved by the implicit Euler method while the Giesekus equation is approximated by the modified Euler

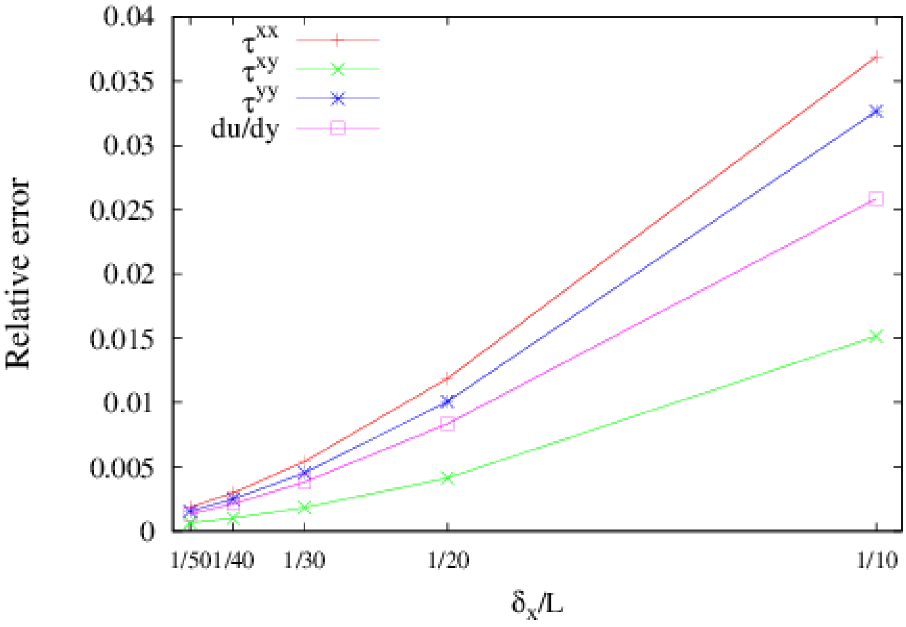


Figure 4. Decrease of the relative errors obtained on the five meshes.

method. An analytic solution for fully developed channel flows was presented. The code validation was performed by simulating the flow in a confined channel and the numerical solutions were compared with the respective analytic solutions. Excellent agreement between the analytic and numerical solutions were displayed. It was shown that the numerical method developed in this work can simulate flows governed by the Giesekus constitutive equation.

## 7. ACKNOWLEDGEMENTS

The authors acknowledge the financial support given by the funding agencies: CNPq - Conselho Nacional de Desenvolvimento Científico e Tecnológico grant No. 306280/2014-0, FAPESP - Fundação de Amparo a Pesquisa do Estado de São Paulo grant No. 2014/21415-7). This work is part of the activities developed within the CEPID-CeMEAI FAPESP project Grant No. $2013/07375-0$.

## 8. REFERENCES

Alves, M. A., Pinho, F. T., and Oliveira, P. J., 2001. "Study of steady pipe and channel flows of a single-mode Phan-Thien-Tanner fluid". *Journal of Non-Newtonian Fluid Mechanics*, Vol. 101, pp. 55–76.

Araujo, M. T., 2015. *Solução numérica do modelo Giesekus para escoamentos bidimensionais com superfícies livres*. Master's Dissertation, Instituto de Ciências Matemáticas e de Computação, USP, São Carlos, SP, Brazil.

Delvaux, V. and Crochet, M. J., 1990. "Numerical simulation of delayed die swell". *Rheologica Acta*, Vol. 29, pp. 1-10.

Harlow, F. H. and Welch, J. E., 1965. "Numerical calculation of time-dependent viscous incompressible flow of fluid with free surface". *Physics Fluids*, Vol. 8, pp. 2182–2189.

Joie, J. and Graebling, D., 2013. "Numerical simulation of polymer flows using non-copnforming finite elements". *Computers & Fluids*, Vol. 79, pp. 178-189.

McKee, S., Tomé, M. F., Ferreira, V. G., Cuminato, J. A., Castelo, A., Sousa, F. S., Mangiavacchi, N., 2008. "The MAC method". *Computers & Fluids*, Vol. 37, pp. 907–930.

Mu, Y., Zhao, G., Chen, A. and Wu, X., 2013. "Modelling and simulation of three-dimensional extrusion swelling of viscoelastic fluids with PTT, Giesekus and FENE-P constitutive models". *International Journal for Numerical Methods in Fluids*, Vol. 72, pp. 846-863.

Oishi, C. M., Martins, F. P., Tomé, M. F., Cuminato, J. A. and McKee, S., 2011. "Numerical solution of the eXtended Pom-Pom model for viscoelastic free surface flows". *Journal of Non-Newtonian Fluid Mechanics*, Vol. 166, pp. 165–179.

Oztekin, A., Brown, R. A. and McKinley, G. H., 1994. "Quantitative prediction of the viscoelastic instability in cone-and-plate flow of a Boger fluid using a multi-mode Giesekus model". *Journal of Non-Newtonian Fluid Mechanics*, Vol. 54, pp. 351-377.

Raisi, A., Mirzazadeh, M., Dehnavi, A. S. and Rashidi, F., 2008. "Approximate solution for the Couette-Poiseuille flow of the Giesekus model between parallel plates". *Rheologica Acta*, Vol. 47, pp. 75-80.

Rajagopalan, D., Armstrong, R. C. and Brown, R. A., 1990. "Finite element methods for calculation of steady viscoelastic flow using constitutive equations with a Newtonian viscosity". *Journal of Non-Newtonian Fluid Mechanics*, Vol. 36, pp. 159–192.

Schleiniger, G. and Weinacht, R. J., 1991. "Steady Poiseuille flows for a Giesekus fluid". *Journal of Non-Newtonian Fluid Mechanics*, Vol. 40, pp. 79–102.

Tomé, M. F., Castelo, A., Cesar, C. N. L., McKee, S. and Cuminato, J. A., 2000. "Freeflow: an integrated simulation system for three-dimensional free surface flows". *Computing and Visualization in Science*, Vol. 2, pp. 199–210.

Tomé, M. F., Mangiavacchi, N., Cuminato, J. A., Castelo, A. and McKee, S., 2002. "A finite difference technique for simulating unsteady viscoelastic free surface flows". *Journal of Non-Newtonian Fluid Mechanics*, Vol. 106, pp. 61–106.

## 9. RESPONSIBILITY NOTICE

The authors are the only responsible for the printed material included in this paper.